KU LEUVEN

STADIUS
Center for Dynamical Systems, Signal Processing and Data Analytics

Citation/Reference	Authors: Sibren Lagauw, Lukas Vanpoucke, Bart De Moor Title: Exact Solution to the Least Squares Realization Problem as a Multiparameter Eigenvalue Problem Journal/Conference/Book: Automatica Vol/Book Chapter: 185 Pages: 112792
Archived version	☐ Submitted version ■ Accepted (Author manuscript: the content is identical to the content of the published paper, but without the final typesetting by the publisher) ☐ Published ☐ Published (Open Access)
Acknowledgements	In this manuscript, the following funding is acknowledged: ☐ EU H22020 ☐ EU Horizon Europe ■ FWO ■ KULeuven Internal Funds ☐ VLAIO ☐ AI ■ ERC ☐ Other
Published version	`https://authors.elsevier.com/sd/article/S0005109825006910`
Copyright statement	CC BY 4.0
Author contact	sibren.lagauw@esat.kuleuven.be lukas.vanpoucke@esat.kuleuven.be bart.demoor@esat.kuleuven.be



Exact Solution to the Least Squares Realization Problem as a Multiparameter Eigenvalue Problem ⋆

Sibren Lagauw *, Lukas Vanpoucke, Bart De Moor [1]

Center for Dynamical Systems, Signal Processing, and Data Analytics (STADIUS), Department of Electrical Engineering (ESAT), KU Leuven, Kasteelpark Arenberg 10, 3001 Leuven, Belgium.

Abstract

We consider the least squares (LS) realization of an autonomous single-output linear time-invariant dynamical model for a given sequence of output data. As opposed to standard system identification practices, which often rely on (heuristic) iterative optimization techniques, we propose an exact solution to this non-convex optimization problem: the *globally optimal* solution(s) are identified by means of a *deterministic* eigenvalue procedure. In particular, we illustrate that for all (local) minimizers, the corresponding misfit can be characterized as the result of filtering an unknown signal twice through a finite-impulse response filter. Exploiting this insight, we propose a novel (rectangular) multiparameter eigenvalue problem (MEP), the eigentuples of which allow to retrieve all local and global minimizers of the identification problem. The proposed MEP is of great theoretical interest and offers new insights into the structure of the LS realization problem, which we explore in detail. We provide numerical examples to illustrate our findings.

Key words: Least squares realization; Multiparameter eigenvalue problem; Global optimization;

1 Introduction

This paper presents novel mathematical insights into the *least squares (LS) realization problem*. While this problem has been extensively studied, the results obtained here were, to the best of our knowledge, previously unknown and have not been documented in the literature.

1.1 Problem formulation

We consider *autonomous single-output linear time-invariant (LTI) causal dynamical models in discrete-time*, with a pre-specified model order n, which corresponds to the number of states. For this model class, output data $\widehat{\boldsymbol{y}} = [\widehat{y}_0 \ \cdots \ \widehat{y}_{N-1}]^\mathsf{T} \in \mathbb{R}^N$ (with $N > 2n$) satisfy a difference equation of the form:

$$\widehat{y}_{k+n} + a_1\widehat{y}_{k+n-1} + \cdots + a_n\widehat{y}_k = a(z)\widehat{y}_k = 0, \qquad (1)$$

where $a(z) = z^n + a_1 z^{n-1} + \cdots + a_n$ is a degree n polynomial in the forward-shift operator z, i.e., $z\widehat{y}_k = \widehat{y}_{k+1}$. The coefficients of $a(z)$ correspond to the parameters $\boldsymbol{a} = [a_n \ a_{n-1} \ \cdots \ a_1]^\mathsf{T} \in \mathbb{R}^n$ of the autonomous LTI model. Data $\widehat{\boldsymbol{y}}$ that satisfy (1) for all $k = 0, \ldots, N-n-1$ will be called *model-compliant* with respect to the model parameters $\boldsymbol{a}$.

The LS realization problem is formulated as follows: given data $\boldsymbol{y} = [y_0 \ \cdots \ y_{N-1}]^\mathsf{T} \in \mathbb{R}^N$, we want to identify the model parameters $\boldsymbol{a}$ that minimize the 2-norm of the so-called misfit $\widetilde{\boldsymbol{y}} = \boldsymbol{y} - \widehat{\boldsymbol{y}}$, which is the modification needed to make the given data $\boldsymbol{y}$ model-compliant:

$$\underset{\boldsymbol{a}\in\mathbb{R}^n,\, \widehat{\boldsymbol{y}}\in\mathbb{R}^N}{\text{minimize}} \quad \frac{1}{2}\left\|\widetilde{\boldsymbol{y}}\right\|_2^2 = \frac{1}{2}\left\|\boldsymbol{y} - \widehat{\boldsymbol{y}}\right\|_2^2, \qquad (2a)$$

$$\text{subject to} \quad a(z)\widehat{y}_k = 0, \ \ \forall k = 0, \ldots, N-n-1. \qquad (2b)$$

This modeling setup is depicted in Fig. 1.

Remark that even though the considered model class is linear in the parameters $\boldsymbol{a}$, it is nonlinear in the unknowns $\boldsymbol{a}$ and $\widehat{\boldsymbol{y}}$ simultaneously. Consequently, the LS realization problem constitutes a *non-convex optimization problem*, implying that (many) local optima can exist (see e.g., Fig. 2).

⋆ A part of the material in this paper was presented at the 22nd European Control Conference [28].

* Corresponding author.

Email addresses: sibren.lagauw@esat.kuleuven.be (Sibren Lagauw), lukas.vanpoucke@esat.kuleuven.be (Lukas Vanpoucke), bart.demoor@esat.kuleuven.be (Bart De Moor).

[1] Fellow IEEE, IFAC, SIAM.

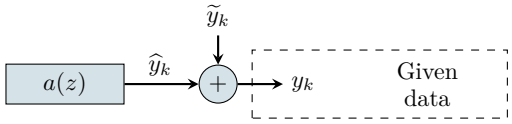

Fig. 1. Schematic representation of the autonomous LTI single-output model. Given data $\boldsymbol{y} \in \mathbb{R}^N$ are to be modified using the so-called misfit $\widetilde{\boldsymbol{y}} \in \mathbb{R}^N$, so that the modified data $\widehat{\boldsymbol{y}} = \boldsymbol{y} - \widetilde{\boldsymbol{y}}$ are model-compliant.

1.2 Contributions and outline

In this paper, we propose an *exact solution* to the LS realization problem: contrary to standard engineering practices (see Section 1.3), we deem the non-convex optimization problem (2) to be mathematically 'solved' if and only if the *globally optimal* model(s) have been identified by means of a *deterministic* procedure.

The main claim and results of this paper are:

(1) We formalize a finite-dimensional version of what is called 'Walsh's Theorem': the optimal misfit is the result of filtering an unknown signal twice by the same finite impulse response (FIR) filter (cf. Theorem 1).
(2) We claim that the exact solution to the LS realization problem is an eigenvalue problem: exploiting the characterization of Theorem 1, we propose a novel, *rectangular multiparameter eigenvalue problem (MEP)*, the set of eigentuples [2] of which contains all local and global minimizers of the problem (cf. Theorem 2). Besides its computational advantages, the novel MEP is also of great theoretical interest, offering new insights into the structure of the LS realization problem.
(3) We demonstrate that, for a subset of the critical points of the problem, the corresponding model-compliant data $\widehat{\boldsymbol{y}}$ have so-called *lower-order dynamics*, and we show that these critical points must be either saddle points or local maximizers of the problem. This eventually leads to the proof of Theorem 2.

The remainder of this paper is organized as follows. We conclude Section 1 by presenting an overview of the background and the key literature relevant to our work. Section 2 recapitulates the two alternative representations for the model dynamics described in [11]. The necessary conditions for first-order optimality are discussed in Section 3, leading to a finite-dimensional version of Walsh's Theorem. Exploiting the results from Sections 2-3, we propose the novel MEP in Section 4 and characterize the so-called 'lower-order' critical points of the LS realization problem in Section 5. Several numerical examples to illustrate the obtained results are provided in Section 6. We conclude the paper in Section 7.

[2] A k-parameter eigenvalue problem has k-tuples of eigenvalues, which we refer to as *eigentuples*.

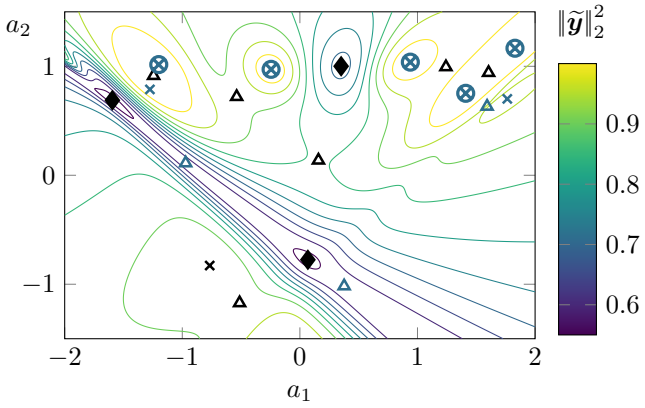

Fig. 2. Contour plot of the objective function of the LS realization problem as a function of the parameters a_1, a_2, illustrating the non-convex nature of the problem. For all values (a_1, a_2), the optimal $\widehat{\boldsymbol{y}}$ was determined via (13) to compute the corresponding objective function value (cf. the formulation in (14)). The problem setup corresponds to Example 2 described in Section 6. Critical points contained in the displayed region are highlighted: local minimizers (♦), saddle points (△) and local maximizers (×), where critical points appearing as eigentuples of the proposed MEP (19) are depicted in black. Local maximizers for which the cost function reaches the global maximum $\|\boldsymbol{y}\|_2^2$ are encircled (⊗). The global minimizer lies outside the displayed region.

1.3 Background and literature overview

The literature about the difference relation (1) and methods to estimate the coefficients from data, from an applied engineering point of view, is vast. The first idea goes back to the French engineer Prony, in 1795 [12], see e.g., [20,21,24] for more information. From a contemporary systems theory point of view, (1) is the characteristic (or minimal) polynomial of a linear system, and hence relates subsequent samples of model-compliant output data from an autonomous LTI system or an LTI impulse response. Therefore, it should come as no surprise that the LS realization problem occurs in a wide variety of data driven engineering fields, such as (we limit ourselves to the most basic references as the literature here is enormous): high-resolution frequency estimation and harmonic retrieval [1,4,5,26] (see [37] for an extensive overview), direction-of-arrival estimation in array processing [19,31,35,38], shape-from-moments problems [15], and realization algorithms for converting impulse response samples into state-space models [22,25,44].

Engineers typically resort to various 'approximate' approaches to efficiently solve the non-convex optimization problem (2). Examples are the iterative quadratic maximum likelihood [29], Steiglitz-McBride [16,33], constrained total least squares [1], the Riemannian SVD [7,8,9,10] and the variable projection method proposed in [18]. In addition to these specialized approaches, plain numerical optimization techniques, such

as those often used in prediction error methods [30] and errors-in-variables methods [36], provide yet another alternative means of solving the problem.

Despite their effectiveness in practice, most of these methods are heuristic in the sense that, due to the non-convex nature of the problem, their performance is often highly sensitive to the initialization, convergence issues can arise, reproducibility of the obtained results is not always guaranteed, and even if some form of optimality is obtained, certification of *global* optimality is generally impossible. Additionally, in a maximum-likelihood setting, a priori probabilistic assumptions are often made on the inaccuracies perturbing the model-compliant data, for instance that they follow a multivariate Gaussian distribution and/or that they are 'white'. While these assumptions can be justified asymptotically for large N, they are heuristic in a finite-sample setting.

The aforementioned approaches stand in marked contrast to our objective, which is to obtain an *exact* solution: a deterministic approach that achieves global optimality. In prior work, various system identification problems have been shown to be essentially an eigenvalue problem [2,40]. These findings are based on the combined insights that the problems in question are polynomial in nature and that global polynomial optimization is equivalent to solving a multiparameter eigenvalue problem (MEP) [13,14].

The MEP generalizes the standard eigenvalue problem by allowing more than one eigenvalue and removing the restriction of linearity in its parameter(s). Consequently, each MEP is inherently connected to a system of multivariate polynomial equations. As a comprehensive treatment of MEPs lies beyond the scope of this text, we refer the interested reader to recent literature [6,23,39]. Efficient numerical algorithms to find all the (real-valued) affine eigentuples of an MEP are available, e.g., the (block) Macaulay framework described in [39,41,42] or the methods from [23,32]. However, the computational complexity involved with solving an MEP grows exponentially with its degree and the dimensions of its coefficient matrices. Accordingly, MEP-based exact solution approaches serve primarily as theoretical benchmarks rather than as practical tools suitable for large-scale problems.

The LS realization problem under consideration was surprisingly only recognized to be an MEP in [11]. Despite the notable theoretical importance of these findings, the obtained MEPs exhibit certain less advantageous characteristics: the size of the coefficient matrices and/or the degree of the MEPs grow fast for increasing problem sizes. By contrast, the MEP that we derive is *cubic* and has significantly more compact coefficient matrices, so that the novel methodology allows us to tackle (relatively) larger examples. The solution set of our MEP differs from that of the MEPs described in [11], as it excludes the so-called lower-order critical points (see Section 5.3), thereby reducing the problem complexity.

The 'double-FIR-filter' property of the optimal misfits, which was noted as a secondary observation in [11], serves as the foundation for the proposed MEP. The property is reminiscent of the interpolatory conditions described in Walsh's Theorem [33, Theorem 3.4], which originates from the field of rational approximation [43]. Our approach is further inspired by our previous work [27], where we leveraged Walsh's Theorem in an infinite-dimensional setting to derive a new methodology for globally optimal single-input single-output H_2-norm model reduction.

2 Model Dynamics

We briefly recapitulate the two alternative representations of the dynamics of a single-output autonomous LTI model described in [11] (Sections 2.1-2.2). Both representations reveal the structure of the model-compliant data $\widehat{\boldsymbol{y}}$, which will be instrumental in Sections 3 and 5.

2.1 Kernel representation

The set of all sequences $\widehat{\boldsymbol{y}} \in \mathbb{R}^N$ that are model-compliant with respect to given model parameters $\boldsymbol{a} \in \mathbb{R}^n$, is referred to as the *behavior* of that model. Writing out the difference equation (1) for all $k = 0, \ldots, N-n-1$, gives

$$\begin{bmatrix} a_n & \cdots & \cdots & a_1 & 1 & 0 & \cdots & 0 \\ 0 & a_n & \cdots & \cdots & a_1 & 1 & \cdots & 0 \\ \vdots & \ddots & \ddots & \ddots & \ddots & \ddots & \ddots & \vdots \\ 0 & \cdots & 0 & a_n & \cdots & \cdots & a_1 & 1 \end{bmatrix} \widehat{\boldsymbol{y}} = \boldsymbol{T}^{\boldsymbol{a}}_{\boldsymbol{N-n}} \widehat{\boldsymbol{y}} = \boldsymbol{0}, \quad (3)$$

indicating that the behavior of the model can be characterized as the n-dimensional kernel (i.e., right null space) of the banded-Toeplitz [3] matrix $\boldsymbol{T}^{\boldsymbol{a}}_{\boldsymbol{N-n}} \in \mathbb{R}^{(N-n)\times N}$. Note that one can replace the constraints (2b) in the LS realization problem by (3).

The matrix-vector product in (3) can be rewritten as

$$\boldsymbol{T}^{\boldsymbol{a}}_{\boldsymbol{N-n}} \widehat{\boldsymbol{y}} = \widehat{\boldsymbol{Y}} \begin{bmatrix} \boldsymbol{a} \\ 1 \end{bmatrix} = \boldsymbol{0}, \quad (4)$$

[3] The super- and subscript denote the generating vector and number of rows of the Toeplitz matrix $\boldsymbol{T}^{\boldsymbol{a}}_{\boldsymbol{N-n}}$, respectively.

where $\widehat{\boldsymbol{Y}} \in \mathbb{R}^{(N-n)\times(n+1)}$ is the Hankel matrix constructed from the elements of $\widehat{\boldsymbol{y}}$,

$$\widehat{\boldsymbol{Y}} = \begin{bmatrix} \widehat{y}_0 & \widehat{y}_1 & \widehat{y}_2 & \cdots & \widehat{y}_n \\ \widehat{y}_1 & \widehat{y}_2 & \widehat{y}_3 & \cdots & \widehat{y}_{n+1} \\ \vdots & \vdots & \vdots & & \vdots \\ \widehat{y}_{N-n-1} & \widehat{y}_{N-n} & \widehat{y}_{N-n+1} & \cdots & \widehat{y}_{N-1} \end{bmatrix}. \tag{5}$$

Hence, given a (sufficiently large) sequence of model-compliant data $\widehat{\boldsymbol{y}}$, one can retrieve the corresponding model parameters $\boldsymbol{a}$ via the kernel of $\widehat{\boldsymbol{Y}}$.

For the optimization problem (2) to be well-defined, the given data must be incompatible with the model class under consideration. That is, the Hankel matrix $\boldsymbol{Y} \in \mathbb{R}^{(N-n)\times(n+1)}$, constructed from the given data $\boldsymbol{y}$ and defined similarly as in (5), is assumed to be of full column rank. Indeed, when this is not the case, one can always find model parameters $\boldsymbol{a}$ for which the given data $\boldsymbol{y}$ lie in the behavior of the model: $\boldsymbol{Y}[\boldsymbol{a}^\mathsf{T},\, 1]^\mathsf{T} = \boldsymbol{T}^{\boldsymbol{a}}_{\boldsymbol{N-n}}\boldsymbol{y} = \boldsymbol{0}$, such that $\widetilde{\boldsymbol{y}} = \boldsymbol{0}$. Since $\boldsymbol{Y}$ is, by construction, not of full column rank when $n < N \leq 2n$, we require $N > 2n$.

2.2 Image representation

Alternatively, the behavior of the autonomous model can be expressed via a Vandermonde matrix, the image of which equals the kernel of $\boldsymbol{T}^{\boldsymbol{a}}_{\boldsymbol{N-n}}$, leading to the so-called *image representation* of the model dynamics. In this case, the behavior is parametrized by the n poles $\{\lambda_i \in \mathbb{C} \,|\, i = 1, \ldots, n\}$ of the model, i.e., the roots of the monic characteristic polynomial $a(z)$:

$$a(z) = \prod_{i=1}^{n} (z - \lambda_i).$$

For real-valued models, complex-valued poles appear in complex-conjugate pairs, e.g., $\lambda_{i,i+1} = \alpha \pm \beta j$ with $\alpha, \beta \in \mathbb{R}$. The model can therefore be parametrized using n real-valued coefficients, as is the case with the kernel representation. For notational convenience, we temporarily assume that the model has simple poles only, i.e., all roots of $a(z)$ have multiplicity one. In this case, each pole λ_i determines a mode $\boldsymbol{\lambda_i} \in \mathbb{C}^N$ that contributes to the behavior of the model:

$$\boldsymbol{\lambda_i} = \begin{bmatrix} 1 & \lambda_i & \lambda_i^2 & \cdots & \lambda_i^{N-1} \end{bmatrix}^\mathsf{T}. \tag{6}$$

This allows us to represent the model-compliant output data $\widehat{\boldsymbol{y}}$ as the following weighted sum,

$$\widehat{\boldsymbol{y}} = \boldsymbol{\Lambda}\widehat{\boldsymbol{x}} = \begin{bmatrix} \boldsymbol{\lambda_1} & \boldsymbol{\lambda_2} & \cdots & \boldsymbol{\lambda_n} \end{bmatrix} \widehat{\boldsymbol{x}}, \tag{7}$$

where $\boldsymbol{\Lambda} \in \mathbb{C}^{N\times n}$ is a Vandermonde matrix and $\widehat{\boldsymbol{x}} \in \mathbb{C}^n$.

The Vandermonde matrix $\boldsymbol{\Lambda}$ is guaranteed to be of full column rank since Vandermonde vectors $\boldsymbol{\lambda_i}$ and $\boldsymbol{\lambda_j}$ generated by different points $\lambda_i \neq \lambda_j$ are linearly independent by construction. If one were to consider poles with multiplicity greater than one, the matrix $\boldsymbol{\Lambda}$ has to be composed using a combination of standard and confluent Vandermonde vectors (see [11] for more details). Also in this case $\boldsymbol{\Lambda}$ is guaranteed to be of full column rank.

Notice that, in contrast to the image representation, the kernel representation conceals the complexity arising from multiple and complex-conjugate poles. Indeed, this parametrization accommodates all cases without requiring modification, which is advantageous from an optimization standpoint. This motivates our choice to employ the kernel representation in formulating our MEP.

3 Characterizing Optimality

Consider the Lagrangian of the LS realization problem,

$$\mathcal{L}(\boldsymbol{a}, \widehat{\boldsymbol{y}}, \boldsymbol{\ell}) = \frac{1}{2}\left\|\boldsymbol{y} - \widehat{\boldsymbol{y}}\right\|_2^2 + \boldsymbol{\ell}^\mathsf{T}\boldsymbol{T}^{\boldsymbol{a}}_{\boldsymbol{N-n}}\widehat{\boldsymbol{y}},$$

where the variables $\boldsymbol{\ell} \in \mathbb{R}^{N-n}$ are Lagrange multipliers. The first-order necessary conditions for optimality of (2) can now be obtained as,

$$\partial\mathcal{L}/\partial\boldsymbol{\ell} = \boldsymbol{T}^{\boldsymbol{a}}_{\boldsymbol{N-n}}\widehat{\boldsymbol{y}} = \boldsymbol{0}, \tag{8a}$$

$$\partial\mathcal{L}/\partial\widehat{\boldsymbol{y}} = \widehat{\boldsymbol{y}} - \boldsymbol{y} + (\boldsymbol{T}^{\boldsymbol{a}}_{\boldsymbol{N-n}})^\mathsf{T}\boldsymbol{\ell} = \boldsymbol{0}, \tag{8b}$$

$$\partial\mathcal{L}/\partial\boldsymbol{a} = (\widehat{\boldsymbol{Y}}|)^\mathsf{T}\boldsymbol{\ell} = \boldsymbol{0}, \tag{8c}$$

where $\widehat{\boldsymbol{Y}}| \in \mathbb{R}^{(N-n)\times n}$ denotes the matrix obtained by removing the rightmost column from $\widehat{\boldsymbol{Y}}$. The solutions $(\boldsymbol{a}, \widehat{\boldsymbol{y}}, \boldsymbol{\ell})$ to the system of equations (8) are the *critical points* of the LS realization problem (2), of which only the real-valued affine ones are relevant for our purposes.

The LS realization problem (2) has a nested structure:

(1) for given data $\boldsymbol{y}$ and an instance of model parameters $\boldsymbol{a}$, find the minimal 2-norm misfit that makes the given data model-compliant with respect to the given model $\boldsymbol{a}$ (inner-minimization);
(2) for given data $\boldsymbol{y}$, the model parameters $\boldsymbol{a}$ are to be optimized so that the optimal misfit obtained from the inner-minimization has a minimal 2-norm.

In what follows, we will illustrate that the optimality conditions (8a)-(8b) lead to a closed-form solution for the inner-minimization, i.e., the optimal data sequences $\widehat{\boldsymbol{y}}$ and $\widetilde{\boldsymbol{y}}$ can be expressed as a function of the given data $\boldsymbol{y}$ and the model parameters $\boldsymbol{a}$ (Section 3.1). The implications of optimality of the model parameters $\boldsymbol{a}$, via (8c), are discussed in Section 3.2.

3.1 Orthogonal decomposition of the ambient space

The relation in (8b) gives

$$\widetilde{\boldsymbol{y}} = (\boldsymbol{T}^{\boldsymbol{a}}_{\boldsymbol{N-n}})^{\mathsf{T}} \boldsymbol{\ell}. \tag{9}$$

The matrix-vector product corresponds to a convolution operation, indicating that the misfit is the result of filtering the signal $\boldsymbol{\ell}$ through the FIR filter defined by $a(z^{-1})$. Combined with (8a), this illustrates that a particular model, defined by its parameters $\boldsymbol{a}$, induces an orthogonal decomposition of the ambient data space $\mathbb{R}^N$: the optimal misfit $\widetilde{\boldsymbol{y}}$ resides in the $(N-n)$-dimensional row space of $\boldsymbol{T}^{\boldsymbol{a}}_{\boldsymbol{N-n}}$, whereas the optimal model-compliant data $\widehat{\boldsymbol{y}}$ lie in the n-dimensional kernel of $\boldsymbol{T}^{\boldsymbol{a}}_{\boldsymbol{N-n}}$. It is a natural consequence that the optimal model-compliant data and misfit are orthogonal: $\widehat{\boldsymbol{y}}^{\mathsf{T}} \widetilde{\boldsymbol{y}} = 0$.

Combining (8a) and (9) leads to

$$\begin{aligned} \partial \mathcal{L} / \partial \boldsymbol{\ell} = \boldsymbol{T}^{\boldsymbol{a}}_{\boldsymbol{N-n}} \widehat{\boldsymbol{y}} = \boldsymbol{T}^{\boldsymbol{a}}_{\boldsymbol{N-n}} (\boldsymbol{y} - \widetilde{\boldsymbol{y}}) = \boldsymbol{0} \\ \iff \boldsymbol{T}^{\boldsymbol{a}}_{\boldsymbol{N-n}} \boldsymbol{y} = \boldsymbol{T}^{\boldsymbol{a}}_{\boldsymbol{N-n}} (\boldsymbol{T}^{\boldsymbol{a}}_{\boldsymbol{N-n}})^{\mathsf{T}} \boldsymbol{\ell}, \qquad (10) \\ \iff \boldsymbol{\ell} = (\boldsymbol{D}^{\boldsymbol{a}}_{\boldsymbol{N-n}})^{-1} \boldsymbol{T}^{\boldsymbol{a}}_{\boldsymbol{N-n}} \boldsymbol{y}, \qquad (11) \end{aligned}$$

where the matrix $\boldsymbol{D}^{\boldsymbol{a}}_{\boldsymbol{N-n}} = \boldsymbol{T}^{\boldsymbol{a}}_{\boldsymbol{N-n}} (\boldsymbol{T}^{\boldsymbol{a}}_{\boldsymbol{N-n}})^{\mathsf{T}}$ is invertible for any choice of $\boldsymbol{a} \in \mathbb{R}^n$. Subsequently, substitution of (11) into (9) gives

$$\widetilde{\boldsymbol{y}} = (\boldsymbol{T}^{\boldsymbol{a}}_{\boldsymbol{N-n}})^{\mathsf{T}} (\boldsymbol{D}^{\boldsymbol{a}}_{\boldsymbol{N-n}})^{-1} \boldsymbol{T}^{\boldsymbol{a}}_{\boldsymbol{N-n}} \boldsymbol{y}, \tag{12}$$

which, using $\widehat{\boldsymbol{y}} = \boldsymbol{y} - \widetilde{\boldsymbol{y}}$, implies that

$$\widehat{\boldsymbol{y}} = \left(\boldsymbol{I} - (\boldsymbol{T}^{\boldsymbol{a}}_{\boldsymbol{N-n}})^{\mathsf{T}} (\boldsymbol{D}^{\boldsymbol{a}}_{\boldsymbol{N-n}})^{-1} \boldsymbol{T}^{\boldsymbol{a}}_{\boldsymbol{N-n}} \right) \boldsymbol{y}. \tag{13}$$

This indicates that, if the model parameters $\boldsymbol{a}$ were known (cf. the inner-minimization), they would uniquely define the corresponding optimal $\boldsymbol{\ell}$, $\widetilde{\boldsymbol{y}}$ and $\widehat{\boldsymbol{y}}$ via (11), (12) and (13), respectively. In particular, the optimal data sequences $\widetilde{\boldsymbol{y}}$ and $\widehat{\boldsymbol{y}}$ are obtained via the orthogonal projection of the given data $\boldsymbol{y}$ onto the linear subspaces defined by the matrix $\boldsymbol{T}^{\boldsymbol{a}}_{\boldsymbol{N-n}}$. The existence of this closed-form solution for the inner-minimization illustrates that the LS realization problem is an instance of a *separable nonlinear LS problem*[4] [17].

Consequently, for given data $\boldsymbol{y}$ and model order n, a critical point $(\boldsymbol{a}, \widehat{\boldsymbol{y}}, \boldsymbol{\ell})$ of (2) is completely determined by its parameter values $\boldsymbol{a}$. From this point onward, whenever referring to specific model parameters $\boldsymbol{a}$, we assume that $\boldsymbol{\ell}$, $\widetilde{\boldsymbol{y}}$ and $\widehat{\boldsymbol{y}}$ are defined as in (11), (12) and (13).

While tangential to our main discussion, observe that substitution of the closed-form solution (12) into the outer problem (2) eliminates the N decision variables $\widehat{\boldsymbol{y}}$, leading to an equivalent, nonlinear, unconstrained optimization problem over the n model parameters $\boldsymbol{a}$ only

$$\underset{\boldsymbol{a} \in \mathbb{R}^n}{\text{minimize}} \ \frac{1}{2} \left\| \widetilde{\boldsymbol{y}} \right\|_2^2 = \frac{1}{2} \boldsymbol{y}^{\mathsf{T}} (\boldsymbol{T}^{\boldsymbol{a}}_{\boldsymbol{N-n}})^{\mathsf{T}} (\boldsymbol{D}^{\boldsymbol{a}}_{\boldsymbol{N-n}})^{-1} \boldsymbol{T}^{\boldsymbol{a}}_{\boldsymbol{N-n}} \boldsymbol{y}. \tag{14}$$

This formulation has been used to construct Fig. 2.

Example 1 *Consider the numerical example described in [11, Section 8.2], where the globally optimal first-order autonomous LTI LS realization is computed for the sequence of given output data*

$$\boldsymbol{y} = \begin{bmatrix} 4 & 3 & 2 & 1 \end{bmatrix}^{\mathsf{T}}.$$

For $n = 1$, the polynomial $a(z)$ from (1) corresponds to $z + a_1$. By (12), the minimal norm misfit associated to the globally optimal solution $a_1 = -0.6764$ (this value will be computed in Section 4) can be obtained via the following orthogonal projection:

$$\widetilde{\boldsymbol{y}} = \begin{bmatrix} -0.1155 \\ 0.2165 \\ 0.1173 \\ -0.2734 \end{bmatrix} = \underbrace{\begin{bmatrix} 0.4326 & -0.3838 & -0.2596 & -0.1756 \\ -0.3838 & 0.7404 & -0.1756 & -0.1187 \\ -0.2596 & -0.1756 & 0.8813 & -0.0803 \\ -0.1756 & -0.1187 & -0.0803 & 0.9457 \end{bmatrix}}_{\boldsymbol{Q}} \begin{bmatrix} 4 \\ 3 \\ 2 \\ 1 \end{bmatrix},$$

where

$$\boldsymbol{Q} = \left[(\boldsymbol{T}^{\boldsymbol{a}}_{\boldsymbol{3}})^{\mathsf{T}} (\boldsymbol{D}^{\boldsymbol{a}}_{\boldsymbol{3}})^{-1} \boldsymbol{T}^{\boldsymbol{a}}_{\boldsymbol{3}} \right]_{a_1 = -0.6764}. \tag{15}$$

The image representation (7) provides an alternative expression for (13). It follows from $\operatorname{null}(\boldsymbol{T}^{\boldsymbol{a}}_{\boldsymbol{N-n}}) = \operatorname{range}(\boldsymbol{\Lambda})$ that if the poles $\{\lambda_i \in \mathbb{C} \,|\, i = 1, \ldots, n\}$ of the model are known, the optimal model-compliant data $\widehat{\boldsymbol{y}}$ can be obtained via the orthogonal projection of $\boldsymbol{y}$ onto the image of $\boldsymbol{\Lambda}$:

$$\widehat{\boldsymbol{y}} = \boldsymbol{\Lambda} [(\boldsymbol{\Lambda})^{\mathsf{H}} \boldsymbol{\Lambda}]^{-1} (\boldsymbol{\Lambda})^{\mathsf{H}} \boldsymbol{y}, \tag{16}$$

where $(\boldsymbol{\Lambda})^{\mathsf{H}}$ denotes the Hermitian conjugate of $\boldsymbol{\Lambda}$.

Example 1 (continued) *The model described by the parameter $a_1 = -0.6764$ has one pole: $\lambda_1 = 0.6764$. It can be verified numerically that*

$$\boldsymbol{Q} = \left[\boldsymbol{I} - \boldsymbol{\lambda} [\boldsymbol{\lambda}^{\mathsf{T}} \boldsymbol{\lambda}]^{-1} \boldsymbol{\lambda}^{\mathsf{T}} \right]_{\lambda_1 = 0.6764},$$

where $\boldsymbol{\lambda} = [1 \ \lambda_1 \ \lambda_1^2 \ \lambda_1^3]^{\mathsf{T}}$ and $\boldsymbol{Q}$ is the matrix from (15).

[4] The 'separability' of the nested optimization problem is a natural property of the LS misfit modeling setup and arises also when more complex model classes are considered, such as multiple-input multiple-output models [34]. It has been exploited by iterative solution approaches, e.g., the alternating LS iterations in [18] and [34, Algorithm 4].

3.2 Optimal model parameters

Taking into account the optimality of the model parameters (8c) illustrates that in a subset of the critical points of (2), the misfit is the result of filtering an unknown signal twice through the FIR filter defined by $a(z^{-1})$.

Theorem 1 (Double FIR filter) *Given a sequence of data $\boldsymbol{y}$, a model order n and a critical point $\boldsymbol{a}$ of (2) for which $\operatorname{rank}(\widehat{\boldsymbol{Y}}) = n$, then the optimal misfit $\widetilde{\boldsymbol{y}}$ can be expressed as,*

$$\widetilde{\boldsymbol{y}} = (\boldsymbol{T}^{\boldsymbol{a}}_{\boldsymbol{N-n}})^{\mathsf{T}}(\boldsymbol{T}^{\boldsymbol{a}}_{\boldsymbol{N-2n}})^{\mathsf{T}}\boldsymbol{g}, \tag{17}$$

for some signal $\boldsymbol{g} \in \mathbb{R}^{N-2n}$, where the matrix $\boldsymbol{T}^{\boldsymbol{a}}_{\boldsymbol{N-2n}} \in \mathbb{R}^{(N-2n)\times(N-n)}$ is a banded Toeplitz matrix defined similarly to the matrix $\boldsymbol{T}^{\boldsymbol{a}}_{\boldsymbol{N-n}}$ from (3).

PROOF. Consider a critical point $\boldsymbol{a}$ and corresponding model-compliant data $\widehat{\boldsymbol{y}}$ obtained via the orthogonal projection (13). Model-compliance of the data ensures that

$$\boldsymbol{T}^{\boldsymbol{a}}_{\boldsymbol{N-2n}}\widehat{\boldsymbol{Y}}| = \boldsymbol{0}.$$

It follows from (4) that $\operatorname{rank}(\widehat{\boldsymbol{Y}}) = n$ implies $\operatorname{rank}(\widehat{\boldsymbol{Y}}|) = n$, such that in this case the rows of the banded Toeplitz matrix $\boldsymbol{T}^{\boldsymbol{a}}_{\boldsymbol{N-2n}}$, which are linearly independent by construction, span the entire $(N-2n)$-dimensional left null space of $\widehat{\boldsymbol{Y}}|$. Combining this insight with (8c) illustrates that there must exist a vector $\boldsymbol{g} \in \mathbb{R}^{N-2n}$ such that,

$$\boldsymbol{\ell} = (\boldsymbol{T}^{\boldsymbol{a}}_{\boldsymbol{N-2n}})^{\mathsf{T}}\boldsymbol{g}. \tag{18}$$

Substituting (18) into (8b) gives the required result.

Example 1 (continued) *The misfit associated to the global minimizer $a_1 = -0.6764$ can be characterized as*

$$\widetilde{\boldsymbol{y}} = \begin{bmatrix} -0.1155 \\ 0.2165 \\ 0.1173 \\ -0.2734 \end{bmatrix} = \left[(\boldsymbol{T}^{\boldsymbol{a}}_{\boldsymbol{3}})^{\mathsf{T}}(\boldsymbol{T}^{\boldsymbol{a}}_{\boldsymbol{2}})^{\mathsf{T}}\right]_{a_1=-0.6764} \underbrace{\begin{bmatrix} -0.2525 \\ -0.2734 \end{bmatrix}}_{\boldsymbol{g}}.$$

Remark that (18) is generally not applicable to critical points $\boldsymbol{a}$ for which $\operatorname{rank}(\widehat{\boldsymbol{Y}}) = m < n$. Indeed, in this case $\operatorname{row}(\boldsymbol{T}^{\boldsymbol{a}}_{\boldsymbol{N-2n}})$ is only a subspace of the $(N-n-m)$-dimensional left null space of $\widehat{\boldsymbol{Y}}|$. This phenomenon is considered in more detail in Section 5.2.

4 Multiparameter Eigenvalue Problem

The characterization of the optimal misfit in Theorem 1 allows us to formulate a *cubic rectangular n-parameter eigenvalue problem (MEP)* in the parameters $\boldsymbol{a}$:

$$\underbrace{\left[\boldsymbol{T}^{\boldsymbol{a}}_{\boldsymbol{N-n}}\boldsymbol{y} \quad \boldsymbol{T}^{\boldsymbol{a}}_{\boldsymbol{N-n}}(\boldsymbol{T}^{\boldsymbol{a}}_{\boldsymbol{N-n}})^{\mathsf{T}}(\boldsymbol{T}^{\boldsymbol{a}}_{\boldsymbol{N-2n}})^{\mathsf{T}}\right]}_{\mathcal{M}(\boldsymbol{a})}\boldsymbol{v} = \boldsymbol{0}, \tag{19}$$

with $\|\boldsymbol{v}\| \neq 0$. The matrix $\mathcal{M}(\boldsymbol{a}) = \sum_{\{\boldsymbol{\alpha}\}} \boldsymbol{M}_{\boldsymbol{\alpha}}\boldsymbol{a}^{\boldsymbol{\alpha}}$, is a third-degree matrix polynomial in the monomials $\boldsymbol{a}^{\boldsymbol{\alpha}} = a_1^{\alpha_1}\cdots a_n^{\alpha_n}$, with coefficient matrices $\boldsymbol{M}_{\boldsymbol{\alpha}} \in \mathbb{R}^{(N-n)\times(N-2n+1)}$, the size of which indicates that (19) is overdetermined when $n > 1$. The values $\boldsymbol{a} \in \mathbb{C}^n$ for which the matrix polynomial $\mathcal{M}(\boldsymbol{a})$ becomes rank-deficient, so that there exists a nonzero vector $\boldsymbol{v} \in \mathbb{C}^{N-2n+1}$ for which these equations are satisfied, are the *affine eigentuples* of this MEP.

The following two results relate the real-valued eigentuples $\boldsymbol{a}$ of the proposed MEP (19) to the critical points of (2). Theorem 2 constitutes our *main contribution*.

Lemma 1 *For given data $\boldsymbol{y}$ and model order n:*

(1) each critical point $\boldsymbol{a}$ for which $\operatorname{rank}(\widehat{\boldsymbol{Y}}) = n$ maps to an affine, real-valued eigentuple of the MEP (19);
(2) each affine, real-valued eigentuple $\boldsymbol{a}$ of the MEP (19) constitutes a critical point of (2).

PROOF. Substitution of (18) into (10) illustrates that for a critical point $\boldsymbol{a}$ of (2) for which the corresponding model-compliant data $\widehat{\boldsymbol{y}}$ satisfy $\operatorname{rank}(\widehat{\boldsymbol{Y}}) = n$, there must exist a vector $\boldsymbol{g} \in \mathbb{R}^{N-2n}$ such that

$$\boldsymbol{T}^{\boldsymbol{a}}_{\boldsymbol{N-n}}\boldsymbol{y} = \boldsymbol{T}^{\boldsymbol{a}}_{\boldsymbol{N-n}}(\boldsymbol{T}^{\boldsymbol{a}}_{\boldsymbol{N-n}})^{\mathsf{T}}(\boldsymbol{T}^{\boldsymbol{a}}_{\boldsymbol{N-2n}})^{\mathsf{T}}\boldsymbol{g}. \tag{20}$$

Bringing everything to the right-hand side and separating out the variables $\boldsymbol{g}$ from (20) into the eigenvector gives (19), with $\boldsymbol{v} = [-1 \;\; \boldsymbol{g}^{\mathsf{T}}]^{\mathsf{T}}$. This proves the first claim.

Secondly, because the matrix $\boldsymbol{T}^{\boldsymbol{a}}_{\boldsymbol{N-n}}(\boldsymbol{T}^{\boldsymbol{a}}_{\boldsymbol{N-n}})^{\mathsf{T}}(\boldsymbol{T}^{\boldsymbol{a}}_{\boldsymbol{N-2n}})^{\mathsf{T}}$ has full column rank for all $\boldsymbol{a} \in \mathbb{R}^n$, there is a one-to-one correspondence between the real-valued affine eigentuples $\boldsymbol{a}$ of the MEP (19) and the real-valued affine common roots $(\boldsymbol{a}, \boldsymbol{g})$ of the system of polynomial equations (20). Indeed, the first element of the eigenvector $\boldsymbol{v}$ of (19) is always nonzero [5], such that the eigenvector $\boldsymbol{v}$ can be appropriately normalized to retrieve $\boldsymbol{g}$. In addition, the matrix obtained after substitution of $\boldsymbol{a}$ into $\mathcal{M}(\boldsymbol{a})$ can drop rank by at most one, such that each eigentuple $\boldsymbol{a}$ has a unique eigenvector $\boldsymbol{v}$ (up to normalization).

[5] If the first element of $\boldsymbol{v}$ equaled zero, then $\boldsymbol{g}$ must be such that $\boldsymbol{T}^{\boldsymbol{a}}_{\boldsymbol{N-n}}(\boldsymbol{T}^{\boldsymbol{a}}_{\boldsymbol{N-n}})^{\mathsf{T}}(\boldsymbol{T}^{\boldsymbol{a}}_{\boldsymbol{N-2n}})^{\mathsf{T}}\boldsymbol{g} = \boldsymbol{0}$. This could only be satisfied for $\boldsymbol{g} = \boldsymbol{0}$, which contradicts $\|\boldsymbol{v}\|_2 \neq 0$.

It now suffices to show that each tuple $(\boldsymbol{a}, \boldsymbol{g})$ satisfying (20) also satisfies (8). If, given such a tuple $(\boldsymbol{a}, \boldsymbol{g})$, $\boldsymbol{\ell}$ is defined as in (11) and $\widehat{\boldsymbol{y}}$ via the orthogonal projection (13), then (8a) and (8b) are satisfied by construction. Multiplication of (20) from the left with $(\boldsymbol{D}^{\boldsymbol{a}}_{\boldsymbol{N-n}})^{-1}$ gives $(\boldsymbol{D}^{\boldsymbol{a}}_{\boldsymbol{N-n}})^{-1}\boldsymbol{T}^{\boldsymbol{a}}_{\boldsymbol{N-n}}\boldsymbol{y} = (\boldsymbol{T}^{\boldsymbol{a}}_{\boldsymbol{N-2n}})^{\mathsf{T}}\boldsymbol{g}$, which, using (11), implies that (8c) is also satisfied.

Theorem 2 *For given data $\boldsymbol{y}$ and model order n, consider the MEP defined in* (19)*. The set of affine, real-valued eigentuples of this MEP contains the model parameters $\boldsymbol{a}$ of all (locally) minimizing critical points, and is therefore guaranteed to include the* global minimizer(s) *of the LS realization problem* (2)*.*

See Section 5.2 for the proof of Theorem 2, which builds on the analysis of lower-order dynamics presented in Lemma 3.

The MEP is polynomial in nature. In the case $n = 1$, the MEP (19) is a polynomial eigenvalue problem (PEP) in the variable a_1 with square coefficient matrices. As such, its eigenvalues correspond to the zeros of the *secular equation*: $\det(\mathcal{M}(\boldsymbol{a})) = 0$, which is a univariate polynomial of degree $3N-5$ in the variable a_1. For $n = 2$, the matrix polynomial $\mathcal{M}(a_1, a_2)$ has dimensions $(N-2)\times(N-3)$, such that its eigentuples could be computed as the common roots of the system of bivariate polynomial equations obtained by equating all maximal minors [6] of that matrix to zero. However, there exist better approaches for obtaining the eigentuples of an MEP. Indeed, it is well established that working with determinants is numerically unfavorable when using finite-precision arithmetic.

The set of (real-valued) affine eigentuples $\boldsymbol{a}$ of the MEP (19) can be computed numerically using the (block) Macaulay framework described in [39,41,42] or the methods from [23,32]. Alternatively, one can obtain the eigentuples of the MEP by computing the set of common roots $(\boldsymbol{a}, \boldsymbol{g})$ of the system of multivariate polynomial equations (20) using off-the-shelf polynomial root-finding techniques, e.g., [3]. Then, the globally optimal solution(s) of the LS realization problem (2) can be selected by evaluating the objective function for each obtained critical point. Note that because (multiparameter) eigenvalue-solvers and polynomial root-finding techniques generally work over the field of complex numbers, the complex-valued eigentuples or common roots have to be pruned away since they have no valid interpretation in the context of the LS realization problem.

Example 1 (continued) *For this example, the system of quartic polynomial equations from* (20) *in the variables* $\{a_1, g_1, g_2\}$ *corresponds to*

$$\begin{cases} 0 = 2a_1g_1 + a_1^2g_2 + a_1^3g_1 - 4a_1 - 3, \\ 0 = g_1 + 2a_1g_2 + 2a_1^2g_1 + a_1^3g_2 - 3a_1 - 2, \\ 0 = g_2 + a_1g_1 + 2a_1^2g_2 - 2a_1 - 1. \end{cases} \tag{21}$$

Observe that the variables $\{g_1, g_2\}$ appear only linearly. Reformulating this system of multivariate polynomial equations gives the following PEP in the parameter a_1:

$$\left(\underbrace{\begin{bmatrix} 3 & 0 & 0 \\ 2 & 1 & 0 \\ 1 & 0 & 1 \end{bmatrix}}_{\boldsymbol{M}_0} + \underbrace{\begin{bmatrix} 4 & 2 & 0 \\ 3 & 0 & 2 \\ 2 & 1 & 0 \end{bmatrix}}_{\boldsymbol{M}_1} a_1 + \underbrace{\begin{bmatrix} 0 & 0 & 1 \\ 0 & 2 & 0 \\ 0 & 0 & 2 \end{bmatrix}}_{\boldsymbol{M}_2} a_1^2 + \underbrace{\begin{bmatrix} 0 & 1 & 0 \\ 0 & 0 & 1 \\ 0 & 0 & 0 \end{bmatrix}}_{\boldsymbol{M}_3} a_1^3 \right) \begin{bmatrix} -1 \\ g_1 \\ g_2 \end{bmatrix} = \boldsymbol{0}. \tag{22}$$

The secular equation of this PEP is given as,

$$\det(\mathcal{M}(a_1)) = 2a_1^7 - 5a_1^6 + 12a_1^5 - a_1^4 + 6a_1^3 + 3a_1^2 + 3 = 0. \tag{23}$$

The seven affine common roots of the system of polynomial equations in (21) *are depicted in Table 1. Computing the affine eigenvalues a_1 of the PEP from* (22) *or computing the roots of the univariate polynomial in* (23) *gives the same results. The set of real-valued eigenvalues corresponds to a singleton: $a_1 = -0.6764$, which is the global minimizer of the LS realization problem. It can be verified numerically that the 3×3 matrix obtained after substitution of $a_1 = -0.6764$ into the matrix polynomial $\mathcal{M}(a_1)$ in* (22) *has rank two.*

Table 1
The affine common roots of the system of polynomial equations in (21) and corresponding cost function values $\|\widetilde{\boldsymbol{y}}\|_2^2$.

$\|\widetilde{\boldsymbol{y}}\|_2^2$	a_1	g_1	g_2
0.149	-0.6764	-0.2525	-0.2734
/	$-0.1589 \mp 0.808j$	$1.3577 \pm 3.8194j$	$1.8359 \pm 3.3491j$
/	$0.4209 \pm 0.6233j$	$3.0425 \mp 2.9959j$	$-0.0785 \pm 1.2013j$
/	$1.3261 \pm 2.0058j$	$-0.2739 \mp 0.6279j$	$0.3793 \mp 0.3849j$

The observation that globally optimal LS realization of autonomous LTI models is an MEP was first shown in [11]. The author starts from the formulation in (14) and illustrates that the first-order necessary conditions for optimality of this unconstrained optimization problem over the model parameters $\boldsymbol{a}$ can be used to construct an MEP [11, Equation (13)]. We will denote this alternative MEP by $\mathcal{M}_{\text{alt}}$. The disadvantage of this approach is that many auxiliary variables have to be introduced to cope with the inverse of the matrix $\boldsymbol{D}^{\boldsymbol{a}}_{\boldsymbol{N-n}}$. As a result, the coefficient matrices of $\mathcal{M}_{\text{alt}}$ tend to grow very large: $((N-n)(n+1)+n) \times ((N-n)(n+1)+1)$, which is

[6] The maximal minors are the $\binom{N-n}{n-1}$ determinants of the submatrices obtained by omitting $n-1$ rows of the $(N-n)\times(N-2n+1)$-sized polynomial matrix $\mathcal{M}(\boldsymbol{a})$.

Table 2
Comparison of the sizes of the coefficient matrices of $\mathcal{M}_{\text{alt}}$, the MEP obtained from [11, Equation (13)], and $\mathcal{M}$, the MEP described in (19), for several combinations of (N, n).

(N, n)	size($\mathcal{M}_{\text{alt}}$)	size($\mathcal{M}$)
$(4, 1)$	7×7	3×3
$(16, 6)$	76×71	10×5
$(50, 8)$	386×379	42×35
$(200, 15)$	2975×2961	185×171

approximately $n + 1$ times larger than the coefficient matrices of (19). This becomes especially noticeable for increasing problem sizes (N, n), see, e.g., Table 2. As the computational complexity involved with solving an MEP depends on the interplay of its degree, the number of parameters, and the size of the coefficient matrices, the smaller coefficient matrices of our novel methodology are favorable from a computational point of view.

5 Model Complexity and Lower Order Models

Theorem 1, which is foundational for the proposed MEP, is contingent on the assumption $\text{rank}(\widehat{\boldsymbol{Y}}) = n$. In this section, we investigate the implications of this assumption. To gain insight into the structure of the problem (2), we start with a formal study of the effects of increasing the model order n. We then consider a special type of models that have so-called *lower order dynamics*, i.e., models for which the optimal model-compliant data is such that $\text{rank}(\widehat{\boldsymbol{Y}}) < n$. The obtained results eventually allow us to prove Theorem 2.

Recall that, for a given set of model parameters $\boldsymbol{a}$, we assume the misfit and model-compliant data to be defined via the orthogonal projections in (12) and (13).

5.1 Increasing the model complexity

Although intuitively clear, we formalize the insight that if the globally optimal solution of (2) has a nonzero misfit $\|\widetilde{\boldsymbol{y}}\|_2 > 0$, increasing the complexity of the to-be-realized model (e.g., $n \to n+1$) results in a strict decrease of the global minimum.

Lemma 2 *For given data $\boldsymbol{y}$ and poles $\{\lambda_i\}_{i=1,\dots,n}$ of an nth order model, we have that*

$$\|\widetilde{\boldsymbol{y}}_{\boldsymbol{n+1}}\|_2 \leq \|\widetilde{\boldsymbol{y}}_{\boldsymbol{n}}\|_2 \neq 0, \tag{24}$$

where $\widetilde{\boldsymbol{y}}_{\boldsymbol{n}}$ is the optimal misfit corresponding to the given nth order model and $\widetilde{\boldsymbol{y}}_{\boldsymbol{n+1}}$ is the optimal misfit corresponding to the $(n+1)$th-order model obtained by adding an arbitrary pole $\lambda_{n+1} \in \mathbb{R}$ to the set of poles[7] of the given nth-order model. Moreover, equality holds in (24) if and only if λ_{n+1} is such that

$$\boldsymbol{y} \perp \left[\boldsymbol{I} - \boldsymbol{\Lambda}[(\boldsymbol{\Lambda})^{\mathsf{H}}\boldsymbol{\Lambda}]^{-1}(\boldsymbol{\Lambda})^{\mathsf{H}}\right]\boldsymbol{\lambda}_{\boldsymbol{n+1}}, \tag{25}$$

where the image of $\boldsymbol{\Lambda} \in \mathbb{C}^{N\times n}$ is the behavior of the nth order model, as defined in (7), and $\boldsymbol{\lambda}_{\boldsymbol{n+1}}$ is the Vandermonde vector (6) defined by the new pole λ_{n+1}.

PROOF. Denote by $\widehat{\boldsymbol{y}}_{\boldsymbol{n}}$ the optimal model-compliant data associated to the given nth-order model and data $\boldsymbol{y}$, and define $\boldsymbol{u}_{\boldsymbol{n+1}} \in \mathbb{R}^N$ as the component of $\boldsymbol{\lambda}_{\boldsymbol{n+1}}$ that lies orthogonal to range($\boldsymbol{\Lambda}$), i.e.,

$$\boldsymbol{u}_{\boldsymbol{n+1}} = \left[\boldsymbol{I} - \boldsymbol{\Lambda}[(\boldsymbol{\Lambda})^{\mathsf{H}}\boldsymbol{\Lambda}]^{-1}(\boldsymbol{\Lambda})^{\mathsf{H}}\right]\boldsymbol{\lambda}_{\boldsymbol{n+1}}.$$

Then, it follows from the orthogonal projection in (16) that if the model order is increased by adding a new pole λ_{n+1} to the model, the new model-compliant data $\widehat{\boldsymbol{y}}_{\boldsymbol{n+1}}$ can be expressed as

$$\widehat{\boldsymbol{y}}_{\boldsymbol{n+1}} = \widehat{\boldsymbol{y}}_{\boldsymbol{n}} + \frac{(\boldsymbol{y} - \widehat{\boldsymbol{y}}_{\boldsymbol{n}})^{\mathsf{H}}\boldsymbol{u}_{\boldsymbol{n+1}}}{(\boldsymbol{u}_{\boldsymbol{n+1}})^{\mathsf{H}}\boldsymbol{u}_{\boldsymbol{n+1}}}\boldsymbol{u}_{\boldsymbol{n+1}}. \tag{26}$$

Since $\boldsymbol{u}_{\boldsymbol{n+1}} \perp \widehat{\boldsymbol{y}}_{\boldsymbol{n}} \in \text{range}(\boldsymbol{\Lambda})$, (26) implies

$$\|\widehat{\boldsymbol{y}}_{\boldsymbol{n+1}}\|_2^2 = \|\widehat{\boldsymbol{y}}_{\boldsymbol{n}}\|_2^2 + \left\|\frac{\boldsymbol{y}^{\mathsf{H}}\boldsymbol{u}_{\boldsymbol{n+1}}}{(\boldsymbol{u}_{\boldsymbol{n+1}})^{\mathsf{H}}\boldsymbol{u}_{\boldsymbol{n+1}}}\boldsymbol{u}_{\boldsymbol{n+1}}\right\|_2^2,$$

which, knowing that $\|\boldsymbol{y}\|_2^2 = \|\widehat{\boldsymbol{y}}_{\boldsymbol{n+1}}\|_2^2 + \|\widetilde{\boldsymbol{y}}_{\boldsymbol{n+1}}\|_2^2$, establishes the first part of the proof. Secondly, since Vandermonde vectors $\boldsymbol{\lambda_i}, \boldsymbol{\lambda_j}$ generated by different points $\lambda_i \neq \lambda_j$ are linearly independent[7], $\boldsymbol{\lambda}_{\boldsymbol{n+1}} \notin \text{range}(\boldsymbol{\Lambda})$. Consequently, the vector $\boldsymbol{u}_{\boldsymbol{n+1}}$ is guaranteed to be nonzero, such that $\widehat{\boldsymbol{y}}_{\boldsymbol{n+1}} = \widehat{\boldsymbol{y}}_{\boldsymbol{n}}$ arises only if (25) is satisfied.

A graphical illustration of the effects of the condition (25) in Lemma 2 is given in Fig. 3.

Corollary 1 *Let*

$$s_n = \min_{\boldsymbol{a}\in\mathbb{R}^n} \boldsymbol{y}^{\mathsf{T}}(\boldsymbol{T}^{\boldsymbol{a}}_{\boldsymbol{N-n}})^{\mathsf{T}}(\boldsymbol{D}^{\boldsymbol{a}}_{\boldsymbol{N-n}})^{-1}\boldsymbol{T}^{\boldsymbol{a}}_{\boldsymbol{N-n}}\boldsymbol{y}$$

correspond to the global minimum for a model order n. Then,

$$s_n \neq 0 \iff s_{n+1} < s_n.$$

PROOF. It follows from Lemma 2 that the set of poles λ_{n+1} for which equality holds in (24), consist of finitely many points. Indeed, by the geometry of the problem

[7] If λ_{n+1} is already a pole of the nth-order model, then $\boldsymbol{\lambda}_{\boldsymbol{n+1}}$ must be taken as the appropriate confluent Vandermonde vector, such that also in this case $\boldsymbol{\lambda}_{\boldsymbol{n+1}} \notin \text{range}(\boldsymbol{\Lambda})$.

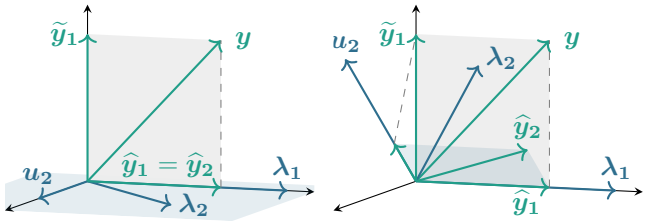

(a) Non-contributing $\boldsymbol{\lambda_2}$ (b) Contributing $\boldsymbol{\lambda_2}$

Fig. 3. Graphical illustration of the two scenarios described in Lemma 2 in the case where a new pole λ_2 is added to an existing first-order model with pole λ_1, with $N = 3$. Within the orthogonal coordinate system (black), the plane depicted in blue corresponds to the behavior of the obtained 2nd order model. The vector $\boldsymbol{u_2}$ is the residual of the orthogonal projection of $\boldsymbol{\lambda_2}$ onto $\boldsymbol{\lambda_1}$, such that $\boldsymbol{u_2} \perp \boldsymbol{\lambda_1}$. The model-compliant data $\widehat{\boldsymbol{y}}_\mathbf{2}$ correspond to the sum of the projection of $\boldsymbol{y}$ onto $\boldsymbol{\lambda_1}$ and the projection of $\widetilde{\boldsymbol{y}}_\mathbf{1}$ onto $\boldsymbol{u_2}$.

($\boldsymbol{y} = \widehat{\boldsymbol{y}}_\boldsymbol{n} + \widetilde{\boldsymbol{y}}_\boldsymbol{n}$ with $\widehat{\boldsymbol{y}}_\boldsymbol{n} \perp \widetilde{\boldsymbol{y}}_\boldsymbol{n}$ and $\widehat{\boldsymbol{y}}_\boldsymbol{n} \in \text{range}(\boldsymbol{\Lambda})$), (25) can be shown to be equivalent to

$$\begin{aligned} &\widetilde{\boldsymbol{y}}_\boldsymbol{n} \perp \left[\boldsymbol{I} - \boldsymbol{\Lambda}[(\boldsymbol{\Lambda})^{\mathsf{H}}\boldsymbol{\Lambda}]^{-1}(\boldsymbol{\Lambda})^{\mathsf{H}}\right]\boldsymbol{\lambda_{n+1}}, \\ \iff\ &\widetilde{\boldsymbol{y}}_\boldsymbol{n} \perp \boldsymbol{\lambda_{n+1}}. \end{aligned} \tag{27}$$

Define $\widetilde{y}_n(z)$ as the $(N-1)$th degree polynomial generated by the nonzero misfit $\widetilde{\boldsymbol{y}}_\boldsymbol{n}$: $\widetilde{y}_n(z) = \widetilde{y}_0 + \widetilde{y}_1 z + \widetilde{y}_2 z^2 + \cdots + \widetilde{y}_{N-1} z^{N-1}$, then (27) is satisfied exclusively by Vandermonde vectors constructed from the roots of this univariate polynomial: for each root λ_i of $\widetilde{y}_n(z)$, $\widetilde{y}_n(\lambda_i) = \boldsymbol{\lambda_i}^{\mathsf{H}}\widetilde{\boldsymbol{y}}_\boldsymbol{n} = 0$ by definition, where we used that complex roots appear in complex-conjugate pairs. Consequently, as long as the misfit $\widetilde{\boldsymbol{y}}_\boldsymbol{n}$ is nonzero, one can always select a value for λ_{n+1} so that (25) does not hold.

Note that when λ_{n+1} is such that (25) is satisfied, the mode $\boldsymbol{\lambda_{n+1}}$ does not contribute to the new model-compliant data. In this case, we can express $\widehat{\boldsymbol{y}}_\boldsymbol{n+1}$ as

$$\widehat{\boldsymbol{y}}_\boldsymbol{n+1} = \begin{bmatrix}\boldsymbol{\lambda_1} & \cdots & \boldsymbol{\lambda_n} & \boldsymbol{\lambda_{n+1}}\end{bmatrix}\begin{bmatrix}\widehat{\boldsymbol{x}} \\ 0\end{bmatrix} = \widehat{\boldsymbol{y}}_\boldsymbol{n}, \tag{28}$$

where we used the image representation from (7). By consequence, the Hankel matrix $\widehat{\boldsymbol{Y}}' \in \mathbb{R}^{N-(n+1)\times n+2}$ constructed from $\widehat{\boldsymbol{y}}_\boldsymbol{n+1}$ is at least rank-two deficient.

5.2 Lower-order dynamics

The derivation leading to (28) provides insight into the structure of models with lower-order dynamics, that is, models for which the optimal model-compliant data is such that $\text{rank}(\widehat{\boldsymbol{Y}}) < n$. Consider such an nth-order model, then it follows from Lemma 2 that

$$\begin{aligned} \text{rank}(\widehat{\boldsymbol{Y}}) < n \iff \exists j \in \{1,\ldots,n\} \mid \\ \boldsymbol{y}^{\mathsf{H}}\left[\boldsymbol{I} - \boldsymbol{\Lambda'}[(\boldsymbol{\Lambda'})^{\mathsf{H}}\boldsymbol{\Lambda'_N}]^{-1}(\boldsymbol{\Lambda'_N})^{\mathsf{H}}\right]\boldsymbol{\lambda_j} = 0, \end{aligned} \tag{29}$$

where $\boldsymbol{\Lambda'_N} \in \mathbb{C}^{N\times(n-1)}$ is the Vandermonde matrix constructed from all but one of the poles $\{\lambda_i\}_{i=1,\ldots,n|i\neq j}$.

Confining our attention to the critical points of the LS realization problem (2), we can use (29) to show that a critical point with lower-order dynamics, such that Theorem 1 might not be applicable for this model, cannot be a locally minimizing solution of (2).

Lemma 3 *Given the parameters $\boldsymbol{a}$ of an nth order model that is a (locally) minimizing critical point of* (2)*, then the corresponding optimal model-compliant data $\widehat{\boldsymbol{y}}$ have exactly nth order LTI dynamics, i.e.,* $\text{rank}(\widehat{\boldsymbol{Y}}) = n$.

PROOF. The proof is by contradiction. Suppose that the model $\boldsymbol{a}$ is a (locally) minimizing critical point of (2), for which the corresponding model-compliant data $\widehat{\boldsymbol{y}}$ have $\text{rank}(\widehat{\boldsymbol{Y}}) < n$. Then, as in (29), the latter implies that at least one of the modes [8], take $\boldsymbol{\lambda_j} \in \mathbb{R}^N$, of the model $\boldsymbol{a}$ does not contribute to the model-compliant data $\widehat{\boldsymbol{y}}$. If we now locally perturb the coefficients of $\boldsymbol{a}$ so that this pole $\lambda_j \to \lambda_{j,\epsilon} = \lambda_j + \epsilon$, with $\epsilon \in \mathbb{R}$ arbitrarily small and so that

$$\boldsymbol{y}^{\mathsf{H}}\left[\boldsymbol{I} - \boldsymbol{\Lambda'}[(\boldsymbol{\Lambda'})^{\mathsf{H}}\boldsymbol{\Lambda'}]^{-1}(\boldsymbol{\Lambda'})^{\mathsf{H}}\right]\boldsymbol{\lambda_{j,\epsilon}} \neq 0,$$

while keeping the other poles of the model unchanged, then, the pole $\lambda_{j,\epsilon}$ will contribute to the obtained model-compliant data $\widehat{\boldsymbol{y}}_\boldsymbol{\epsilon}$.

By Lemma 2, the misfit $\widetilde{\boldsymbol{y}}_\boldsymbol{\epsilon}$ of this novel model, which is arbitrarily close to the given lower-order model, is guaranteed to have a smaller 2-norm than the misfit $\widetilde{\boldsymbol{y}}$ associated to the parameters $\boldsymbol{a}$. In other words, it is possible to locally perturb the model parameters $\boldsymbol{a}$ so that the objective function value decreases, which contradicts the assumption that the lower-order model defined by $\boldsymbol{a}$ is a (local) minimizer. This completes the proof.

Lemma 3 implies that critical points of the LS realization problem (2) with lower-order dynamics need to correspond to saddle points or (local) maximizers. Extreme examples of these lower-order critical points are

[8] We assume for simplicity that the pole λ_j is real-valued. The proof, however, can easily be generalized to the complex-valued case: if λ_j is complex-valued, then also the mode corresponding to the complex conjugate $\overline{\lambda_j}$ does not contribute to the model-compliant data $\widehat{\boldsymbol{y}}$. In this case, both modes $\boldsymbol{\lambda_j}$ and $\overline{\boldsymbol{\lambda_j}}$ have to be perturbed simultaneously.

the *global maximizers* of the LS realization problem (14). For these model parameters $\boldsymbol{a}$, the given data $\boldsymbol{y}$ lie completely in the row space of $\boldsymbol{T}^{\boldsymbol{a}}_{\boldsymbol{N-n}}$, such that the orthogonal projections from (12) and (13) result in $\widetilde{\boldsymbol{y}} = \boldsymbol{y}$ and $\widehat{\boldsymbol{y}} = \boldsymbol{0}$, respectively.

Proof of Theorem 2 The claim is a direct consequence of Lemma 1 and Lemma 3.

Note that (18) and consequently Theorem 1 are generically [9] not satisfied for these lower-order critical points. Consider for example the above-mentioned global maximizers: in this case $\operatorname{rank}(\widehat{\boldsymbol{Y}}) = 0$, such that the optimality constraint (8c) does not put any restriction on the vector $\boldsymbol{\ell}$. As such, these lower order critical points are generally not included in the set of eigentuples of the proposed MEP (19), since the derivation of the MEP is contingent on the characterization given in Theorem 1.

Example 1 (continued) *Consider the model* $a_1 = 1.6506$*, which is a global maximizer of the LS realization problem* (14)*. For this parameter value,*

$$\boldsymbol{y} = \begin{bmatrix} 4 & 3 & 2 & 1 \end{bmatrix}^{\mathsf{T}} \in \operatorname{row}(\boldsymbol{T}^{\boldsymbol{a}}_{\boldsymbol{3}}|_{a_1=1.6506}),$$

such that the misfit $\widetilde{\boldsymbol{y}}$ *obtained with the projection* (12) *is equal to the given data:* $\widetilde{\boldsymbol{y}} = \boldsymbol{y}$*. One can verify numerically that the characterization in* (17) *from Theorem 1 does not hold for this global maximizer:*

$$\widetilde{\boldsymbol{y}} = \boldsymbol{y} = \begin{bmatrix} 4 & 3 & 2 & 1 \end{bmatrix}^{\mathsf{T}} \notin \operatorname{range}(\left[(\boldsymbol{T}^{\boldsymbol{a}}_{\boldsymbol{3}})^{\mathsf{T}}(\boldsymbol{T}^{\boldsymbol{a}}_{\boldsymbol{2}})^{\mathsf{T}}\right]_{a_1=1.6506}).$$

5.3 Computation of all critical points

As the MEP $\mathcal{M}_{\text{alt}}$ from [11] does not exploit Theorem 1—it follows directly from the first-order necessary conditions for optimality (8)—its real-valued eigentuples are in one-to-one correspondence to the set of all critical points of (2). This is in contrast to the proposed MEP (19), for which we know from Section 5.2 that some saddle points and/or maximizers of the problem do not appear as eigentuples. As such, $\mathcal{M}_{\text{alt}}$ could be advantageous if one is interested in obtaining a complete characterization of the search space. However, this also implies that one can expect the number of (real-valued) eigentuples of $\mathcal{M}_{\text{alt}}$ to be significantly larger than for the proposed MEP. To substantiate this claim, consider the following example. Define $y(z)$ as the polynomial generated by the given data $\boldsymbol{y}$: $y(z) = y_0 + y_1 z + y_2 z^2 + \cdots + y_{N-1} z^{N-1}$. To each root λ_i of $y(z)$, corresponds a Vandermonde vector $\boldsymbol{\lambda_i}$ such that $\boldsymbol{y}^{\mathsf{T}}\boldsymbol{\lambda_i} = 0$. As such, by selection of n roots from $y(z)$ as the poles of a model, one can construct $\binom{N-1}{n}$ models for which $\widehat{\boldsymbol{y}}$ obtained via (13) is the zero vector. The parameters of each of these models will appear as a (possibly complex-valued [10]) eigentuple of the MEP $\mathcal{M}_{\text{alt}}$. A similar argument can be made to characterize the number of lower-order critical points with $\operatorname{rank}(\widehat{\boldsymbol{Y}}) = m$, where $0 < m < n$.

Example 1 (continued) *When we use the MEP* $\mathcal{M}_{alt}$ *from [11, Equation (13)] for* $\boldsymbol{y} = [4, 3, 2, 1]^{\mathsf{T}}$ *and* $n = 1$*, 10 affine eigenvalues* a_1 *are retrieved, 7 of which correspond to the affine eigenvalues of the PEP* (22) *depicted in Table 1. The three additional eigenvalues* $\{1.6506, 0.1747 \pm 1.5469j\}$ *correspond to the roots of the polynomial:* $y(z) = 4 + 3z + 2z^2 + z^3$*. The model with* $a_1 = 1.6506$ *is a global maximizer of* (14)*.*

6 Numerical Examples

We consider several numerical examples to illustrate the results of Section 4. Numerical values are rounded for displaying purposes. A MATLAB implementation of the (block) Macaulay method [39,41,42], available online at `www.macaulaylab.net`, has been used to compute the eigentuples of the obtained MEPs.

Example 2 *In this example we fit a second-order model* ($n = 2$) *to given data* $\boldsymbol{y}$ ($N = 16$) *with* $\|\boldsymbol{y}\|_2^2 = 1.0323$*:*

$$\begin{aligned}\boldsymbol{y} = [&-0.3845, -0.2211, -0.1000, -0.1976, -0.6810,\\ &-0.1417, -0.2469, -0.0766, -0.0595, 0.2074, 0.0506,\\ &-0.1412, 0.0690, 0.2549, -0.0975, -0.2959]^{\mathsf{T}}.\end{aligned}$$

The MEP (19) *has 739 affine eigentuples, 15 of which are real-valued (see Table 3). The globally optimal solution* $\boldsymbol{a} = [9.7392, -12.692]^{\mathsf{T}}$ *has an objective function value approximately equal to* 0.4985*. Notice from Table 3 that the matrix* $\widehat{\boldsymbol{Y}}$ *corresponding to each critical point is of rank* n*, indicating that no lower-order critical points are retrieved (cf. the discussion in Section 5.2). The globally optimal model-compliant data* $\widehat{\boldsymbol{y}}$ *are depicted in Fig. 4. The objective function value for model parameters* (a_1, a_2) *in the interval* $[-2, 2] \times [-1.5, 1.5]$ *and corresponding critical points are depicted in Fig. 2. Notice that only a subset (including all minimizers) of the critical points appear as eigentuples of the proposed MEP* (19)*.*

[9] Even though these lower-order critical points do not satisfy (17) when generic data $\boldsymbol{y}$ are used, nothing forbids them to 'coincidentally' do so. One can easily construct such an example: take an arbitrary set of model parameters $\boldsymbol{a}$ and construct the data $\boldsymbol{y}$ as $\boldsymbol{y} = (\boldsymbol{T}^{\boldsymbol{a}}_{\boldsymbol{N-n}})^{\mathsf{T}}(\boldsymbol{T}^{\boldsymbol{a}}_{\boldsymbol{N-2n}})^{\mathsf{T}}\boldsymbol{f}$ for some $\boldsymbol{f} \in \mathbb{R}^{2N-n}$. Then, for this sequence $\boldsymbol{y}$, $\boldsymbol{a}$ is a global maximizer of (14), corresponding to the 0th order solution $\widehat{\boldsymbol{y}} = \boldsymbol{0}$, which nevertheless satisfies (18).

[10] When $y(z)$ has complex-valued roots, a subset of the $\binom{N-1}{n}$ models will have complex-valued parameters $\boldsymbol{a}$. Such a 'complex-valued' model has no valid interpretation in the context of the identification problem (2).

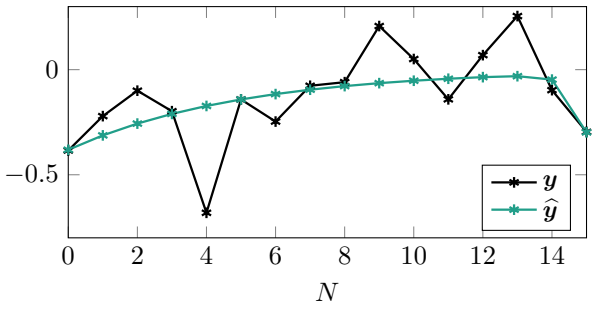

Fig. 4. The given data $\boldsymbol{y}$ and optimal model-compliant data $\widehat{\boldsymbol{y}}$ corresponding to the global minimizer of Example 2.

Table 3
The objective function value and poles λ_i for the critical points (a_1, a_2) of Example 2 obtained using the MEP from (19). The rightmost column depicts the next to smallest singular value of the Hankel matrix constructed from $\widehat{\boldsymbol{y}}$, illustrating that none of the retrieved models have lower-order dynamics (cf. Section 5.2).

$\|\widetilde{\boldsymbol{y}}\|_2^2$	a_1	a_2	$\{\lambda_1, \lambda_2\}$	$\sigma_n(\widehat{\boldsymbol{Y}})$
0.4985	−12.692	9.7392	11.871, 0.8204	0.2361
0.5328	−1.5946	0.6882	$0.7973 + 0.2292j$	0.1605
0.5381	0.0679	−0.7755	−0.9153, 0.8473	0.2786
0.6846	0.3508	1.0007	$-0.1754 \pm 0.9849j$	0.5499
0.8478	−11.632	−11.401	12.541, −0.9091	0.2809
0.8479	0.1578	0.1371	$-0.0789 \pm 0.3618j$	0.1563
0.8697	−7.9710	−5.1738	8.5744, −0.6034	0.2718
0.9118	−0.5376	0.7206	$0.2688 \pm 0.8052j$	0.2696
0.9134	−2.7291	3.4371	$1.3646 \pm 1.2550j$	0.1560
0.9139	−0.5126	−1.1719	1.3688, −0.8561	0.2378
0.9147	16.548	23.256	−14.998, −1.5506	0.2023
0.9271	−0.7668	−0.8285	1.3711, −0.6043	0.2278
0.9829	1.2420	0.9939	$-0.6210 \pm 0.7799j$	0.2388
1.0293	1.6045	0.9413	$-0.8023 \pm 0.5456j$	0.0428
1.0308	−1.2470	0.9175	$0.6235 \pm 0.7271j$	0.0396

Example 3 *We fit models for $n = 1, 2, 3, 4, 5$ to a sequence of given data $\boldsymbol{y}$ ($N = 10$) that is generated by a fifth-order autonomous LTI model with poles $(0.5, 0.25 \pm 0.75j, -0.3 \pm 0.5j)$:*

$$\begin{aligned}\boldsymbol{y} = [&-0.0001, -0.0963, 0.8035,\\ &2.1025, -1.0864, -1.2530, 0.1556,\\ &0.6388, 0.2978, -0.2089]^{\mathsf{T}}.\end{aligned}$$

The objective function value of the globally optimal model and the number of real-valued affine eigentuples of the MEP are depicted in Table 4. For $n = 5$, the MEP has one real-valued eigentuple. It corresponds to the model parameters that were used to generate $\boldsymbol{y}$, i.e., the coefficients of the fifth-degree polynomial:

$$\begin{aligned}a(z) = &(z - 0.5)(z - 0.25 + 0.75j)\\ &(z - 0.25 - 0.75j)(z + 0.3 + 0.5j)(z + 0.3 - 0.5j).\end{aligned}$$

The number of real-valued affine eigentuples n_a peaks at $n = 3$, after which it decreases as n approaches the model order with which the given data has been generated. The model-compliant data corresponding to the globally optimal solution(s) $\{\widehat{\boldsymbol{y}}_{\boldsymbol{n}}\}_{n=1,\ldots,5}$ are depicted in Fig. 5.

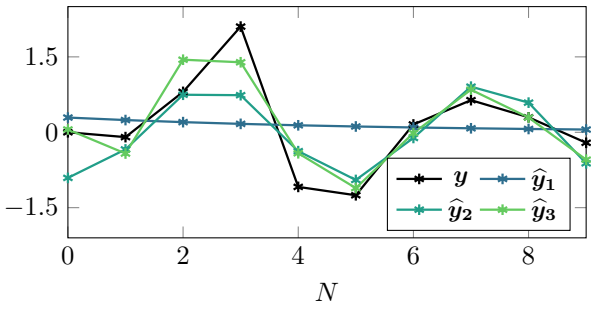

Fig. 5. The given data $\boldsymbol{y}$ and the globally optimal model-compliant data $\widehat{\boldsymbol{y}}$ corresponding to the globally optimal solution(s) of Example 3. Note that $\boldsymbol{y} = \widehat{\boldsymbol{y}}_{\boldsymbol{5}} \approx \widehat{\boldsymbol{y}}_{\boldsymbol{4}}$.

Table 4
The global minimum and the number of real-valued affine eigentuples n_a corresponding to $n = 1, 2, \ldots, 5$ in Example 3.

n	1	2	3	4	5
$\|\widetilde{\boldsymbol{y}}\|_2^2$	8.12	3.74	1.68	6.06×10^{-4}	$\mathcal{O}(10^{-31})$
n_a	5	10	17	13	1

Example 4 *We fit a third-order model ($n = 3$) to given data $\boldsymbol{y}$ ($N = 30$), which is constructed as:*

$$\boldsymbol{y} = \boldsymbol{y}_{\mathbf{3rd}} + \alpha \cdot \texttt{randn(N,1)}, \tag{30}$$

where $\alpha = 1.5$ and $\boldsymbol{y}_{\mathbf{3rd}}$ is generated by a third-order model with poles $\{1.1, 0.5 \pm 0.9j\}$ and initial conditions: $y_{3\mathrm{rd},0} = 1$, $y_{3\mathrm{rd},1} = 0$, $y_{3\mathrm{rd},2} = 1.5$. To make the results reproducible, the random number generator used by MATLAB's `randn()` *function was seeded via* `rng(10)`*. Solving the system of equations (20) using the software package*[11] *from [3] allows us to retrieve 45 critical points. The parameter values of (some of) these critical points are depicted in Table 5. The global minimizer has an objective function value of $\|\widetilde{\boldsymbol{y}}\|_2^2 = 41.309$ (compared to $\|\boldsymbol{y}\|_2^2 = 7574.04$). The obtained data sequence is visualized in Fig. 6.*

Based on the objective function values, the set of critical points can be divided into two groups: 25 points for which $225 < \|\widetilde{\boldsymbol{y}}\|_2^2 < 255$; and 20 critical points with objective

[11] Contrary to the block Macaulay method [39], homotopy continuation methods can exploit *parallelism* in the computations, allowing to tackle larger problems.

Table 5
The objective function value and the dominant pole (pair) λ_{d} for (some of) the critical points (a_1, a_2, a_3) of Example 4, obtained using the system of polynomial equations from (20).

$\|\widetilde{\boldsymbol{y}}\|_2^2$	a_1	a_2	a_3	λ_{d}	
41.309	−2.091	2.120	−1.132	1.100	25 critical points
225.73	−1.079	0.950	−1.084	1.106	
⋮					
251.56	1.063	−1.217	−1.307	1.106	
253.94	−0.215	0.023	−1.113	1.105	
7504.5	−1.443	0.420	0.147	$0.820 \pm 0.267j$	20 critical points
7507.0	−1.870	1.124	−0.172	$0.8189 \pm 0.271j$	
⋮					
7566.3	0.458	0.691	−0.128	$-0.310 \pm 0.834j$	
7567.4	1.395	0.546	−0.150	$-0.788 \pm 0.458j$	

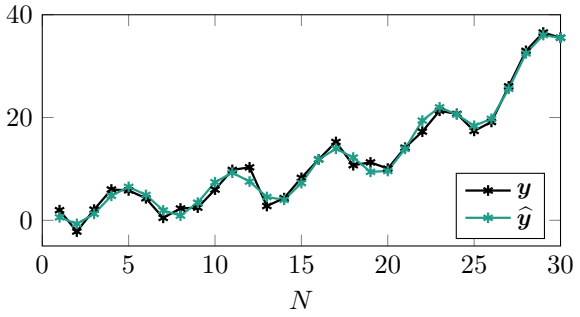

Fig. 6. The given data $\boldsymbol{y}$ and the globally optimal model-compliant data $\widehat{\boldsymbol{y}}$ corresponding to the globally optimal solution of Example 4.

function value close to the global maximum $\|\boldsymbol{y}\|_2^2$. Interestingly, Fig. 7 shows that the critical points of the first and second group approximately lie on a plane in the ambient space $\mathbb{R}^3$. Closer observation learns that this plane spans all the coefficients of third-order monic polynomials $a(z)$ for which (at least) one of the roots equals 1.1, which is the dominant pole[12] *of the model used to generate $\boldsymbol{y}_{\mathbf{3rd}}$. This 'clustering effect' of the critical points arises due to the high signal-to-noise level present in the given data $\boldsymbol{y}$. The effect becomes less outspoken when the example is repeated for larger values of α in* (30).

7 Conclusions and Future Work

Least squares (LS) realization of autonomous single-output linear time-invariant dynamical models, despite being a well-established topic in the statistical and system identification literature, remained partially unresolved in terms of its *exact* solution. We propose an exact

[12] The dominant pole (pair) of a model $\boldsymbol{a}$ corresponds to the root(s) of $a(z)$ with the largest magnitude.

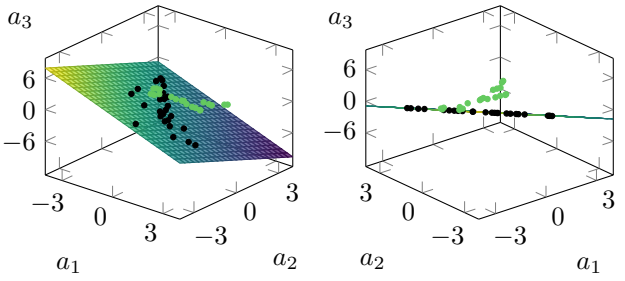

Fig. 7. Scatter plots of the parameters values (a_1, a_2, a_3) of the critical points of Example 4. The critical points depicted in black (green) have an objective function value for which $\|\widetilde{\boldsymbol{y}}\|_2^2 < 255$ (resp. $\|\widetilde{\boldsymbol{y}}\|_2^2 > 7500$). The plane depicts all parameter values for which (at least) one of the roots of the polynomial $a(z) = z^3 + a_1 z^2 + a_2 z + a_3$ is equal to 1.1. The plots illustrate that the best-performing critical points have one pole approximating the dominant pole of the model used to generate the data $\boldsymbol{y}$.

solution, that is, a *deterministic* procedure that identifies the *global minimizer(s)* of the (non-convex) optimization problem. This objective is fundamentally different from the standard engineering practice, in which one typically resorts to (heuristic) iterative optimization techniques and/or invokes asymptotic statistical assumptions about the given data to obtain a 'sufficiently good' solution, as efficiently as possible.

As demonstrated in this work, the exact solution of the LS realization problem can be formulated as a rectangular multiparameter eigenvalue problem (MEP). The MEP is a generalization of the standard eigenvalue problem, where more than one eigenvalue is allowed and the restriction of linearity in its parameter(s) is removed.

Ultimately, we combined general principles from systems theory and optimization, such as first-order optimality conditions, with problem-specific insights (e.g., the 'double-FIR-filter' property) to obtain our results. This paradigm is undoubtedly relevant beyond the immediate context of this particular LS realization problem. More broadly, we demonstrated that MEPs constitute an effective framework for characterizing the critical points of a (highly) non-convex estimation problem.

Recognizing that the computational difficulty involved with solving the obtained MEP grows exponentially with the problem size (N, n), more research is needed to make our theoretical findings applicable in practice. In future work, we will try to exploit the fact that we are only interested in the real-valued eigentuples of the MEP. We also want to perform more numerical examples to get better insights into the nature of the local/global minimizer(s) of the LS realization problem, pushing the problem size (N and/or n) to be as large as possible.

Another challenge considers the number of critical points. In the special case $n = 1$, finiteness of the affine

solution set of the proposed MEP is easily proved via its secular equation. However, even though in all of our numerical examples the set of affine eigentuples of the MEP has been zero-dimensional—it consists of a finite number of isolated elements—finiteness of the affine solution set for all (N, n) remains to be proven.

Acknowledgements

This work was supported in part by the KU Leuven Research Fund (projects iBOF/24/064 and IDN/24/013), the Industrial Research Fund and several LRD bilateral industrial projects; in part by the Flemish Government agencies: FWO (TBM T001725N), EWI through the Flanders AI Research Program and VLAIO (CSBO - HBC.2021.0076); and in part by the European Commission (ERC Adv. Grant) under Grant 885682. Views and opinions expressed are however those of the author(s) only and do not necessarily reflect those of the European Union or ERC. Neither the European Union nor the granting authority can be held responsible for them. The work of S. Lagauw was supported by the FWO Fundamental Research Fellowship under Grant 11K5625N. The authors acknowledge Christof Vermeersch for the development of the MacaulayLab toolbox and his support in the creation of the visualizations included in this paper. We thank Katrien De Cock for her meticulous proofreading of the manuscript.

References

[1] T. J. Abatzoglou, J. M. Mendel, and G. A. Harada. The constrained total least squares technique and its applications to harmonic superresolution. *IEEE Transactions on Signal Processing*, 39(5):1070–1087, 1991.

[2] K. Batserlier, P. Dreesen, and B. De Moor. Prediction error method identification is an eigenvalue problem. *IFAC Proceedings Volumes*, 45(16):221–226, 2012. 16th IFAC Symposium on System Identification.

[3] P. Breiding and S. Timme. HomotopyContinuation.jl: A package for homotopy continuation in Julia. In *Mathematical Software – ICMS 2018*, pages 458–465. Springer International Publishing, 2018.

[4] Y. Bresler and A. Macovski. Exact maximum likelihood parameter estimation of superimposed exponential signals in noise. *IEEE Transactions on Acoustics, Speech, and Signal Processing*, 34(5):1081–1089, 1986.

[5] J. A. Cadzow. Signal enhancement: A composite property mapping algorithm. *IEEE Transactions on Acoustics, Speech, and Signal Processing*, 36(1):49–62, 1988.

[6] K. De Cock and B. De Moor. Multiparameter eigenvalue problems and shift-invariance. *IFAC-PapersOnLine*, 54(9):159–165, 2021. Proceedings of MTNS 2020.

[7] B. De Moor. Structured total least squares and L_2 approximation problems. *Linear Algebra and its Applications*, 188–189:163–205, 1993.

[8] B. De Moor. Total least squares for affinely structured matrices and the noisy realization problem. *IEEE Transactions on Signal Processing*, 42(11):3104–3113, 1994.

[9] B. De Moor. *SVD and Signal Processing III*, chapter The Riemannian Singular Value Decomposition, pages 61–78. Algorithms, Architectures and Applications. Elsevier, 1995.

[10] B. De Moor. *Recent Advances in Total Least Squares Techniques and Errors-in-Variables Modeling*, chapter Linear System Identification, Structured Total Least Squares and the Riemannian SVD, pages 225–238. SIAM, 1997.

[11] B. De Moor. Least squares optimal realisation of autonomous LTI systems is an eigenvalue problem. *Communications in Information and Systems*, 20(2):163–207, 2020.

[12] G. C. F. M. R. de Prony. Essai expérimental et analytique, etc. *Journal de l'Ecole Polytechnique de Paris*, 1:24–76, 1795.

[13] P. Dreesen, K. Batselier, and B. De Moor. Back to the roots: Polynomial system solving, linear algebra, systems theory. *IFAC Proceedings Volumes*, 45(16):1203–1208, 2012. 16th IFAC Symposium on System Identification.

[14] P. Dreesen and B. De Moor. *Model-Based Control: Bridging Rigorous Theory and Advanced Technology*, chapter Polynomial Optimization Problems are Eigenvalue Problems, pages 49–68. Springer US, 2009.

[15] M. Elad, P. Milanfar, and G. H. Golub. Shape from moments—an estimation theory perspective. *IEEE Transactions on Signal Processing*, 52(7):1814–1829, 2004.

[16] N. Everitt, M. Galrinho, and H. Hjalmarsson. Open-loop asymptotically efficient model reduction with the Steiglitz-McBride method. *Automatica*, 89:221–234, 2018.

[17] G. H. Golub and V. Pereyra. The differentiation of pseudo-inverses and nonlinear least squares problems whose variables separate. *SIAM Journal on Numerical Analysis*, 10(2):413–432, 1973.

[18] G. H. Golub and V. Pereyra. Separable nonlinear least squares: The variable projection method and its applications. *Inverse Problems*, 19(2):R1–R26, 2003.

[19] M. Haardt. Structured least squares to improve the performance of ESPRIT-type algorithms. *IEEE Transactions on Signal Processing*, 45(3):792–799, 1997.

[20] J. F. Hauer, C. J. Demeure, and L. L. Scharf. Initial results in Prony analysis of power system response signals. *IEEE Transactions on Power Systems*, 5(1):80–89, 1990.

[21] F. B. Hildebrand. *Introduction to Numerical Analysis*, pages 457–462. Dover Publications, New York, 2nd edition, 1974.

[22] B. L. Ho and R. E. Kalman. Effective construction of linear, state-variable models from input/output functions. *Regelungstechnik*, 14:545–548, 1966.

[23] M. E. Hochstenbach, T. Košir, and B. Plestenjak. Numerical methods for rectangular multiparameter eigenvalue problems, with applications to finding optimal ARMA and LTI models. *Numerical Linear Algebra with Applications*, 31(2), 2024.

[24] J. N. Holt and R. J. Antill. Determining the number of terms in a Prony algorithm exponential fit. *Mathematical Biosciences*, 36(3–4):319–332, 1977.

[25] S. Y. Kung. A new identification and model reduction algorithm via singular value decomposition. In *Proceedings of the 12th Asilomar Conference on Circuits, Systems and Computers, Institute of Electrical and Electronics Engineers, New York*, pages 705–714, 1978.

[26] S. Y. Kung, K. S. Arun, and D. V. Bhaskar Rao. State-space and singular-value decomposition-based approximation methods for the harmonic retrieval problem. *Journal of the Optical Society of America*, 73(12):1799–1811, 1983.

[27] S. Lagauw, O. M. Agudelo, and B. De Moor. Globally optimal SISO H_2-norm model reduction using Walsh's Theorem. *IEEE Control Systems Letters*, 7:1670–1675, 2023.

[28] S. Lagauw, L. Vanpoucke, and B. De Moor. Exact characterization of the global optima of least squares realization of autonomous LTI models as a multiparameter eigenvalue problem. In *2024 European Control Conference (ECC)*, pages 3446–3451, 2024.

[29] P. Lemmerling, L. Vanhamme, S. Van Huffel, and B. De Moor. IQML-like algorithms for solving structured total least squares problems: a unified view. *Signal Processing*, 81:1935–1945, 2001.

[30] L. Ljung. *System Identification: Theory for the User*. Information and System Sciences Series. Prentice-Hall, Upper Saddle River, NJ, USA, 2nd edition, 1999.

[31] A. R. Paulraj, R. Roy, and T. Kailath. A subspace rotation approach to signal parameter estimation. *Proceedings of the IEEE*, 74(7):1044–1046, 1986.

[32] B. Plestenjak. MultiParEig (`https://www.mathworks.com/matlabcentral/fileexchange/47844-multipareig`), MATLAB central file exchange. Retrieved Nov. 12, 2025.

[33] P. A. Regalia. *Adaptive IIR Filtering in Signal Processing and Control*. Marcel Dekker Inc., New York, NY, 1995.

[34] B. Roorda and C. Heij. Global total least squares modeling of multivariable time series. *IEEE Transactions on Automatic Control*, 40(1):50–63, January 1995.

[35] R. Roy and T. Kailath. ESPRIT-estimation of signal parameters via rotational invariance techniques. *IEEE Transactions on Acoustics, Speech, and Signal Processing*, 37(7):984–995, 1989.

[36] T. Söderström. *Errors-in-variables Methods in System Identification*. Communications and Control Engineering (CCE). Springer Cham, 2018.

[37] P. Stoica and R. L. Moses. *Spectral Analysis of Signals*. Pearson Prentice Hall, 2005.

[38] P. Stoica and K. C. Sharman. Maximum likelihood methods for direction-of-arival estimation. *IEEE Transactions on Acoustics, Speech, and Signal Processing*, 38(7):1132–1143, 1990.

[39] C. Vermeersch. *The (Block) Macaulay Matrix: Solving Systems of Multivariate Polynomial Equations and Multiparameter Eigenvalue Problems*. PhD thesis, Faculty of Engineering, KU Leuven, Leuven, Belgium, 2023.

[40] C. Vermeersch and B. De Moor. Globally optimal least-squares ARMA model identification is an eigenvalue problem. *IEEE Control Systems Letters*, 3(4):1062–1067, 2019.

[41] C. Vermeersch and B. De Moor. Two complementary block Macaulay matrix algorithms to solve multiparameter eigenvalue problems. *Linear Algebra and its Applications*, 654:177–209, 2022.

[42] C. Vermeersch and B. De Moor. Two double recursive block Macaulay matrix algorithms to solve multiparameter eigenvalue problems. *IEEE Control Systems Letters*, 7:319–324, 2023.

[43] J. L. Walsh. *Interpolation and Approximation by Rational Functions in the Complex Domain*. American Mathematical Society, 3rd edition, 1960.

[44] H. Zeiger and A. McEwen. Approximate linear realizations of given dimension via Ho's algorithm. *IEEE Transactions on Automatic Control*, 19(2):153–153, 1974.